



Aalborg Universitet

AALBORG UNIVERSITY
DENMARK

Investigating stimulation parameters for preferential small fiber activation using exponentially rising electrical currents

Hugosdottir, Rosa; Mørch, Carsten Dahl; Andersen, Ole K; Arendt-Nielsen, Lars

Published in:
Journal of Neurophysiology

DOI (link to publication from Publisher):
[10.1152/jn.00390.2019](https://doi.org/10.1152/jn.00390.2019)

Publication date:
2019

Document Version
Accepted author manuscript, peer reviewed version

[Link to publication from Aalborg University](#)

Citation for published version (APA):

Hugosdottir, R., Mørch, C. D., Andersen, O. K., & Arendt-Nielsen, L. (2019). Investigating stimulation parameters for preferential small fiber activation using exponentially rising electrical currents. *Journal of Neurophysiology*, 122(4), 1745-1752. <https://doi.org/10.1152/jn.00390.2019>

General rights

Copyright and moral rights for the publications made accessible in the public portal are retained by the authors and/or other copyright owners and it is a condition of accessing publications that users recognise and abide by the legal requirements associated with these rights.

- ? Users may download and print one copy of any publication from the public portal for the purpose of private study or research.
- ? You may not further distribute the material or use it for any profit-making activity or commercial gain
- ? You may freely distribute the URL identifying the publication in the public portal ?

Take down policy

If you believe that this document breaches copyright please contact us at vbn@aub.aau.dk providing details, and we will remove access to the work immediately and investigate your claim.

1 **Investigating stimulation parameters for preferential small fiber**
2 **activation using exponentially rising electrical currents.**

3 Authors: Rosa Hugosdottir, Carsten Dahl Mørch, Ole Kæseler Andersen, and Lars
4 Arendt-Nielsen

5 Center of Neuroplasticity and Pain, SMI, Department of Health Science and Technology, Aalborg University

6 Corresponding author information: Carsten Dahl Mørch, email address: cdahl@hst.aau.dk

7 Abstract

8 Electrical stimulation is widely used in pain research and profiling but current technologies lack selectivity
9 towards small sensory fibers. Pin electrodes deliver high current density in upper skin layers and it has been
10 proposed that slowly rising exponential pulses can elevate large fiber activation threshold and thereby increase
11 preferential small fiber activation. Optimal stimulation parameters for the combined pin electrode and
12 exponential pulse stimulation have so far not been established as is the aim of this study. Perception thresholds
13 were compared between pin- and patch electrodes using single 1-100 ms exponential- and rectangular pulses.
14 Stimulus-response functions were evaluated for both pulse shapes delivered as single pulses and pulse trains of
15 10 Hz using intensities from 0.1-20 times perception threshold. Perception thresholds (mA) decreased when
16 duration was increased for both electrodes with rectangular pulses and also for the pin electrode with exponential
17 pulses. For the patch electrode, perception thresholds for exponential pulses decreased for durations ≤ 10 ms, but
18 increased for durations ≥ 15 ms, indicating accommodation of large fibers. Stimulus-response curves for single
19 pulses were similar for the two pulse shapes. For pulse trains, the slope of the curve was higher for rectangular
20 pulses. Maximal large fiber accommodation to exponential pulses was observed for 100 ms pulses, indicating
21 that 100 ms exponential pulses should be applied for preferential small fiber activation. Intensity of 10 times

22 perception threshold was sufficient to cause maximal pain ratings. The developed methodology may open new
23 opportunities for using electrical stimulation paradigms for small fiber stimulation and diagnostics.

24 **New and noteworthy**

25 Selective activation of small cutaneous nerve fibers is pivotal for investigations of the pain system. The present
26 study demonstrated that patch electrode perception thresholds increase with increased duration of exponential
27 currents from 20- to 100 ms. This is likely caused by large fiber accommodation, which can be utilized to
28 activate small fibers preferentially through small-diameter pin electrodes. This finding may be utilized in studies
29 of fundamental pain mechanisms and e.g. in small fiber neuropathy.

30 **1. Introduction**

31 Selective activation of small fibers could be useful in various applications such as bladder function restoration
32 (Brindley and Craggs 1980), and in pain research (Inui and Kakigi 2012) and pain diagnostics (Hennings et al.
33 2017). However, selective activation of small nerve fibers is difficult since the pain sensing primary afferents
34 have smaller diameters than tactile afferent skin fibers. Electrical stimulation with standard surface patch
35 electrodes activates large diameter fibers at lower intensities than small fibers (Grill and Mortimer 1995). With
36 electrical stimulation, the fiber recruitment order is based on two principles: 1) distance from electrode to the
37 fibers and 2) fiber diameter (Grill and Mortimer 1995). Both of these likely affect the transmembrane potential.
38 Special intra-epidermal (Inui et al. 2002) and cutaneous pin electrodes (Klein et al. 2004; Lelic et al. 2012;
39 Mørch et al. 2011) have been developed to activate the small A δ - and C-fibers preferentially by “isolating” the
40 electrical field in the upper skin layers where primarily small fibers terminate (Ebenezer et al. 2007; Hilliges et
41 al. 1995; Provitera et al. 2007). With short rectangular pulses at intensities close to perception threshold, evoked
42 potential latencies in the A δ -fiber range have been reported for intra-epidermal and pin electrode stimulation
43 (Lelic et al. 2012; Mouraux et al. 2010). At higher intensities, co-activation of larger diameter fibers cannot be
44 excluded (Mouraux et al. 2010). Another approach for targeting small fibers is to utilize the membrane kinetics
45 of the voltage sensitive ion channels. The rate of fiber inactivation is slower than the rate of activation (Grill and

46 Mortimer 1995; Hill 1936; Kugelberg 1944) and by slow depolarization of the membrane, inactivation can be
47 initiated, and thus increasing the activation threshold (accommodation) (Baker and Bostock 1989; Bostock et al.
48 1998; Hennings et al. 2017; Hill 1936; Kugelberg 1944; Li and Bak 1976; Sassen and Zimmermann 1973). The
49 distribution of the different ion channel subtypes, with varying inactivation rates differs between small- and large
50 fibers (Amaya et al. 2000; Blair and Bean 2002; Djouhri et al. 2003; Fang et al. 2002). Extensive depolarization
51 can be obtained with linearly increasing currents (Hennings et al. 2005a; Lucas 1907) and the shape of the
52 depolarizing pulse can be even further improved by applying a slowly rising pulse with an increasing form of an
53 exponential decay (exponential), since the accommodation depends on the current gradient (Hill 1936;
54 Hugosdottir et al. 2017; Lucas 1907). Perception thresholds of sensory cutaneous nerve fibers were recently
55 compared between different slowly rising pulse shapes of 50 ms duration and the above mentioned exponential
56 pulse showed largest ratio between activation of large- and small fibers indicating preferential small fiber
57 activation (Hugosdottir et al. 2017).

58 The combined application of high current density delivered through a pin electrode and slowly raising pulses has
59 not been studied in details and optimal stimulation duration and -intensity remain unknown. In a previous study,
60 at least 2-fold increase in thresholds was found when pin electrode stimulation was applied to skin exposed to
61 lidocaine, which partially blocks the small fibers (Hoberg et al. 2019). This indicated that stimulus intensity
62 above the activation threshold of small fibers is likely needed to depolarize- and accommodate large fibers with
63 slowly increasing pulses. The requirement of using low intensity for selective activation of superficial small
64 fibers may therefore only apply for short duration stimuli (Mouraux et al. 2010), making this electrode-
65 parameter combination highly appealing for use in experimental pain studies where usually higher intensity is
66 needed (spatial recruitment). However, the intensity should be examined carefully, since there might be a narrow
67 range of large fiber accommodation without activation.

68 In this study, perception thresholds to patch- and pin electrodes were assumed to indicate activation of large- and
69 small fibers, respectively. Perception thresholds were obtained for both electrodes to create strength-duration
70 curves for exponential- and rectangular pulses. The aim was to investigate the pulse duration of a single

71 exponential pulse that caused greatest large fiber accommodation while concurrently activated small fibers.
72 Furthermore, the pain response was compared between short rectangular and long duration exponential pulses
73 delivered with the pin electrode at varying stimulus intensities for single pulse and repetitive stimulation.

74 **2. Methods**

75 This study consisted of two experimental sessions performed with approximately two months in between.

76 **Subjects**

77 25 healthy individuals (12 females; 19-30 year; mean age 23.6 years) participated in both experiments (A and B)
78 but one was excluded from Experiment B due to early state pregnancy. All subjects gave their written informed
79 consent to participation in the experiments which was approved by the local ethical committee (N-20160076).
80 The experiment was performed according to the declaration of Helsinki.

81 **Experimental setup**

82 In both experiments, subjects were seated in an inclined hospital bed with their arms resting on pillows. A
83 voltage controlled electrical current stimulator (DS5; Digitimer Ltd; Welwyn Garden City, UK) was used to
84 deliver electrical pulses to the volar forearm of the participants. Stimulation was controlled by the experimenter
85 via a custom-made program (LabVIEW, National Instruments) on a personal computer and a data acquisition
86 card (USB-6351; National instruments). In experiment A, two types of electrodes were used (Fig. 1). A pin
87 electrode was used to activate small A δ - and C-fibers (Klein et al. 2004; Lelic et al. 2012). 15 short circuited
88 small diameter (0.2 mm) stainless steel pins were placed in a circle with a diameter of 10 mm and used as
89 cathodes. The anode was a concentric stainless-steel ring, with an inner diameter of 22 mm and an outer
90 diameter of 36 mm. A standard patch electrode was used to activate mainly the large A β -fibers. The cathode was
91 a 15 mm x 20 mm Ag-AgCl electrode (Neuroline 700, Ambu A/S, Ballerup, Denmark) and the anode was a
92 large 5 cm x 9 cm patch (Pals Neurostimulation electrode, Axelgaard, Co., Ltd., Fallbrook, CA, USA).

93 *Figure 1. The electrodes used in the experiment. Left) Pin electrode is composed of 15 small cathodal pins and a*
94 *concentric anode. Right) The patch electrode cathode.*

95

96 **Pulse shapes**

97 Two pulse shapes were applied: 1) rectangular- and 2) exponential pulse (i.e. an increasing form of exponential
98 decaying current which was bounded to a maximal stimulation current, Fig. 2, Eq. 1).

$$i(t) = \begin{cases} \frac{I_s}{1 - e^{-\frac{T_s}{\tau}}} \left(1 - e^{-\frac{t}{\tau}}\right), & 0 \leq t < T_s \\ I_s \cdot e^{-\frac{t}{\tau}}, & T_s \leq t \leq T_{tr} \end{cases}$$

99 *Equation 1. Mathematical expression of the stimulation current $i(t)$ for the exponential pulse is shown. I_s = stimulation*
100 *current intensity, T_s = stimulation duration, τ = time constant of current increase = $T_s/2$. Trailing phase: $T_{tr} = T_s * 1.4$*
101 *and $\tau_{tr} = \tau/6.6$.*

102

103 *Figure 2. Examples of the shape of the exponential pulse are shown for durations of 1, 5, 50, and 100 ms. The illustrations*
104 *show the proportion of the maximal stimulation current intensity.*

105 At short durations, the rate of current increase of the exponential pulse was high and thus similar for both pulse
106 shapes, but as the duration increased, the time constant of current increase (τ) for the exponential pulse increased
107 according to $2\tau = T_s$. The exponential pulse had a decaying phase to avoid anodal break excitation, see Fig. 2
108 (Burke and Ginsborg 1956; Hennings et al. 2005c). All pulses were followed with no inter-phase delay by a
109 pulse phase of opposite polarity of same duration and shape, but with amplitude scaled to half the amplitude of
110 the stimulating phase (not shown in illustration of pulses in Fig. 2 and Eq. 1). The pulses were therefore charge
111 imbalanced, but this configuration limited the charge delivered in one direction to avoid skin damage (Merrill et

112 al. 2005). Prior to the experiment, the shapes of the pulses when stimulating a resistor and a capacitor in parallel
113 were verified on an oscilloscope.

114 **Experimental protocol**

115 **Experiment A**

116 Experiment A consisted of two randomized crossover sessions with a short break in between. First, either a pin-
117 or a patch electrode (see Fig. 1) was randomized to be placed on either the right- or left volar forearm. The
118 cathodes of the pin- and patch electrodes were placed 5 cm distal to the cubital fossa. The anode for the patch
119 electrode was placed on the dorsal forearm. The arm and the electrode were then switched in the second session.

120 *Strength-duration curves:* In each session, perception thresholds (see sec: Perception thresholds) were obtained
121 for single rectangular pulses with durations of 1, 5, 50, and 100 ms and single exponential pulses with durations
122 of 1, 5, 10, 15, 20, 30, 40, 50, 60, 80, 100 ms for both electrodes to create strength-duration curves. The order of
123 all pulse forms and durations were randomized.

124 **Experiment B**

125 In experiment B, electrical stimulation was only delivered with the pin electrode, which was placed 5 cm distal
126 to the cubital fossa on the same arm as the subjects had received stimulation with the pin electrode in experiment
127 A.

128 Perception thresholds were initially identified (see sec: Perception thresholds) for a single exponential pulse of
129 40 ms, and a rectangular pulse of 1 ms.

130 *Stimulus response curves:* Both pulse shapes were delivered as single pulses and pulse trains of 10 Hz for 1 s at
131 intensities of 0.1, 0.5, 1, 2, 3, 4, 6, 8, 10, 15, 20 times perception threshold. The stimulation paradigms delivered
132 in experiment B will be referred to as follows: 1) Exponential single pulse, 2) rectangular single pulse, 3)

133 exponential pulse train, and 4) rectangular pulse train. For each paradigm and intensity, the subjects were asked
134 to rate the pain on a numerical rating scale (NRS) from 0-10. The order of the paradigm was first randomized
135 and the order of the delivered intensity was randomized within each paradigm. The long duration pulse of 40 ms
136 was selected for being able to deliver pulse trains of 10 Hz as previously has been applied in experimental pain
137 studies with the pin electrode (Xia et al. 2016a, 2016b).

138 **Perception thresholds**

139 The perception threshold was found using the following staircase procedure (method of limits): The intensity
140 was initially set to 20 μ A for the pin electrode and 200 μ A for the patch electrode. Single pulses were delivered
141 at 0.5 Hz and the intensity of each pulse increased by 5% compared to previous pulse until the subject perceived
142 the stimulation and pressed a handheld custom-made button. Single pulses were again delivered from 110% of
143 the perceived intensity, which then decreased by 5% until the perception dissipated and the subject pressed the
144 button again. Stimulation intensity was thereafter decreased to 90 % of intensity when perception dissipated and
145 the procedure was repeated. The perception threshold was calculated as the average of the three intensities where
146 perception was indicated and three intensities when perception dissipated. A training sequence of this staircase
147 procedure was initially carried out in order to familiarize the subjects with the procedure and the sensation of
148 electrical stimulation.

149 **Data analysis**

150 **Experiment A**

151 Data analyses was performed using MATLAB (R2017b) and SPSS 25, (IBM). The perception threshold
152 representing the current strength in the strength-duration curves were normalized to the rheobase value and then
153 log transformed prior to the statistical analysis.

154 *Strength-duration curves:* The strength-duration relations between pulse duration, electrode, and pulse shape
155 were analyzed by a three-way linear mixed model (LMM). The model had the electrode (pin- and patch

156 electrode), pulse shape (rectangular and exponential), and duration (1, 5, 10, 50, 100 ms) as repeated fixed
157 factors. A random intercept for a subject- and electrode- specific variable was included, and to investigate the
158 effect of habituation, the order in which the pulses were given was added to the model as a covariate. Due to
159 unequal correlation between repeated measures the autoregressive (AR(1)) covariance structure was used. This
160 model was selected based on the lowest Akaike information criterion. In case of a three-way interaction between
161 the fixed factors, 2 x 2 LMM was used to analyze the effect of electrode and pulse shape for each of the five
162 durations. The latter model accounted for the same random intercept, covariate and repeated measure as the
163 three-way model. The strength-duration relationship for the rectangular pulse shape was analyzed by fitting the
164 data to Weiss law for calculating the rheobase and chronaxie for both electrode types (Weiss 1901). The
165 rheobase and chronaxie were compared between the paradigms by using a Friedman test in accordance with the
166 data distribution.

167 Another analysis was carried out to investigate the perception threshold for the exponential pulse shape in more
168 details. This model was a two-way LMM with the electrode type (pin and patch electrode) and pulse duration (1,
169 5, 10, 15, 20, 30, 40, 50, 60, 80, 100 ms) as fixed-effect factors. The same random intercept, covariate, and
170 repeated measures were included as in previously described models. A two-way factorial interaction between the
171 electrode and pulse duration was analyzed to investigate the difference in strength-duration relation between the
172 electrodes. Furthermore, a factor-covariate interaction was analyzed between electrode and stimulation order to
173 investigate the effect of habituation between the electrode types. The part of the strength-duration curve, which
174 manifested a linear relationship between perception threshold (multiple of rheobase) and stimulation duration
175 (T_S) was used to calculate the slope of accommodation. The duration was first transformed to the time constant
176 of current increase (τ) according to: $\tau = T_S/2$, since the accommodation slope is defined as the relative threshold
177 increase with respect to time constant of current increase (rheobase/ τ) (Kugelberg 1944).

178 **Experiment B**

179 *Stimulus-response curves:* The stimulus-response curves were analyzed by fitting the data for each paradigm to
180 sigmoidal curves, according to the following equation: $y(x) = \frac{c}{1+e^{a(b-x)}}$, where a was the slope of the curve, b
181 was the stimulation factor for inducing 50% of maximum pain rating, and c was the maximum pain rating. The
182 coefficients were considered statistically significant different between the paradigms in case of non-overlapping
183 95% confidence intervals.

184 **3. Results**

185 **Experiment A**

186 The strength-duration curves for both pulse shapes are shown for the patch- and the pin electrodes in Fig. 3. The
187 LMM revealed a three-way interaction between the pulse shape, electrode, and duration ($F(4,213.11) = 10.49$, p
188 < 0.001). Two-way interactions were observed for the two long durations (50 and 100 ms). For 50 ms and 100
189 ms, a larger perception threshold difference was observed between the patch- and the pin- electrode for the
190 exponential pulse than for the rectangular pulse (Fig. 3). For the shorter durations, the threshold relations were
191 not statistically different for the two pulse shapes and electrodes.

192

193 *Figure 3. Re-transformed perception threshold normalized to rheobase (mean \pm standard error) vs. pulse*
194 *duration is shown for a) the patch electrode and b) the pin electrode. Asterisk indicate interactions between*
195 *pulse shape and electrode for the specific durations, * $p < 0.05$, ** $p < 0.01$. Exp = Exponential, Rec =*
196 *rectangular.*

197 The raw strength-duration curves for the rectangular pulse used to estimate the rheobase and chronaxie for both
198 electrodes are shown in Fig. 4. The rheobases and chronaxies are presented as median with interquartile range
199 (IQR) for both electrodes in a table, which is included in Fig. 4. A larger rheobase was found for the patch
200 electrode than for the pin electrode (Wilcoxon signed rank test, $p < 0.001$) and a larger chronaxie was found for
201 the pin electrode than for the patch electrode (Wilcoxon signed rank test, $p < 0.001$).

202

203 *Figure 4. Strength-duration curves (on the left) for the rectangular pulse were used to estimate the rheobase and*
204 *chronaxie, which are presented as median and interquartile range in the table on the right. The perception*
205 *threshold in mA on the y-axis of the strength-duration curve was used to represent the current strength needed*
206 *for activation at different durations with the pin- and the patch electrodes.*

207 A more detailed strength-duration curve for the exponential pulse is shown in Fig. 5. Analysis of these curves
208 revealed an interaction between the pulse duration and electrode, $F(10,474.12) = 23.87$, $p < 0.001$ (Fig. 5). This
209 interaction is explained by different strength-duration curves for the two electrode types. For the pin electrode,
210 perception threshold decreased with increased duration, whereas a V-shaped strength-duration relation was
211 observed for the patch electrode (accommodation curve, Fig. 5); The nadir of the curve was reached at 10 ms,
212 followed by increase in perception threshold for longer durations. With respect to the 1 ms pulse duration, the
213 interaction term was significant from 20-100 ms ($p < 0.001$), with an increased effect for the longer durations.
214 The accommodation slope was calculated for the durations, which manifested a linear relationship from Fig. 5
215 (left) ($10 \text{ ms} < t < 60 \text{ ms}$) and transformed to be reported as rheobase/ τ . The accommodation slope was $23.52 \pm$
216 2.84 rheobase/s.

217 Examination of the effect of habituation revealed a significant main effect of stimulation order, $F(1,435.55) =$
218 193.21 , $p < 0.001$. Furthermore, an interaction between stimulation order and electrode was found, $F(1,435.55) =$
219 72.26 , $p < 0.001$. This indicates that the perception threshold increased throughout the session and habituation
220 affected the pin electrode to a greater extent than the patch electrode.

221 The variance due to the subject-and electrode specific intercept contributed profoundly to the model and
222 accounted for 62.3% of the total variance. The standard deviation of the residuals from the LMM was higher for
223 the pin electrode than for the patch electrode (log values: 0.14 and 0.06, respectively).

224

225 *Figure 5. Re-transformed perception thresholds normalized to rheobase (mean ± standard error) are shown for*
226 *all durations of the exponential pulse for the patch electrode on the left and the pin electrode on the right.*
227 *Asterisk indicate statistically significant interaction between electrode and duration for the pin electrode and t =*
228 *1 ms as reference. ** p < 0.01, *** p < 0.001.*

229 **Experiment B**

230 The pain ratings to stimulus of different intensities are shown in Fig. 6. In Tab. 1, coefficients of the fitting to
231 sigmoidal-curve are shown. Similar maximum pain ratings were found for the pulse train stimulation of
232 exponential– and rectangular pulse, which was higher than for single pulses. Lower intensity was needed to
233 cause half of the maximum pain for rectangular pulse train compared to the other paradigms. This is related to
234 the slope, which was also found to be steepest for the rectangular pulse train.

235

236 *Figure 6. Stimulus-response curves are shown for all paradigms. Pain ratings are shown as mean ± standard*
237 *error. The fit for sigmoidal curve with 95% confidence interval is added to the plots.*

238

239 *Table 1. Sigmoidal model fit for the pain ratings (NRS). Model coefficients are shown (with 95% confidence*
240 *interval)*

241

242 **4. Discussion**

243 This study investigated the strength-duration relationship for an exponentially increasing current delivered to
244 human skin for activating sensory afferent fibers. The current strength needed to activate large- and small fibers
245 was indicated by the subjective perception threshold of a standard patch- and pin electrode, respectively. The
246 results showed an increase in perception threshold of the patch- but not pin electrode when long duration

247 exponential current was applied. The increase in perception threshold was maximized for 100 ms duration. For
248 the pin electrode, the strength-duration relation was similar for rectangular and exponential currents. The ability
249 of the exponential pulse to elevate the threshold of the patch electrode exclusively, indicated that this stimulation
250 shape at long durations caused accommodation of large fibers. Therefore, long duration exponential pulses
251 enabled activation of small fibers with limited large fiber activation, especially when applied by the pin
252 electrode. The study furthermore showed that the stimulus-response curves were similar for single long
253 exponential and short rectangular pulses, but the slope of the curves were different for repetitive stimulation.

254 **Neuronal Accommodation**

255 Slowly rising depolarizing pulses have been used in earlier animal (Li and Bak 1976; Sassen and Zimmermann
256 1973) and human studies (Hennings et al. 2005a; Kugelberg 1944) to depolarize the nerve fiber membrane and
257 inactivate mainly the large fibers to achieve preferential small fiber activation. The increase in perception
258 threshold with the patch electrode in present study is an indication of accommodation of large sensory nerve
259 fibers to the long duration exponential pulses ($T_s \geq 20$ ms, see Fig. 5). To compare the rate and degree of
260 accommodation to earlier findings by Kugelberg et al. 1944 it was necessary to transform the pulse duration (T_s)
261 to time constant of current increase (τ), according to $T_s = 2 \tau$. The accommodation slope in the interval of 10 ms
262 $< T_s < 60$ ms was 23.53 ± 2.84 rheobase/s (see Fig. 5), which is comparable to motor neuron accommodation
263 (21.2 ± 0.46 rheobase/s), calculated for $\tau < 100$ ms in the study by Kugelberg and colleagues (Kugelberg 1944).
264 Motor nerves have been shown to accommodate more rapidly than sensory fibers (Bretag and Stämpfli 1975)
265 and maximum threshold increase is usually higher as accommodation breakdown of motor- and sensory fibers
266 has been observed at 2.5-5 and 1.5-2 times rheobase strength, respectively (Kugelberg 1944). The degree of
267 accommodation in the present study was ~ 1.9 times rheobase for the longest duration ($T_s = 100$ ms). A small
268 degree of accommodation breakdown was noticed, but the perception threshold increased to some degree for the
269 longest duration but not at the same increase rate as between 20 ms and 60 ms. It is expected that the perception
270 threshold would not have increased further had durations > 100 ms been included, due to accommodation

271 breakdown (Hennings et al. 2005b; Kugelberg 1944). In another study on motor nerves, similar rate- and degree
272 of accommodation was reported for linearly increasing current (Hennings et al. 2005a). However, the strength-
273 duration curve showed a delayed accommodation initiating at duration of 50 ms (Hennings et al. 2005a)
274 compared to 20 ms duration in the current study. This is further supported in a recent study, where
275 accommodation was indicated for 50 ms exponential pulses (identical to the pulse shape in the present study),
276 but not for linear pulses (Hugosdottir et al. 2017). The exponential pulse therefore produces relatively good
277 accommodation in large sensory fibers, matching the degree and rate of increase when motor fibers are exposed
278 to linear pulses (Hennings et al. 2005a). Taken together previous data and data from the present study,
279 substantial accommodation of large sensory neurons can be obtained with exponential pulses of 20 ms-100 ms,
280 with a maximum for 100 ms pulses. Sinusoidal currents of 5 Hz have been proposed to activate pain sensing
281 fibers (Koga et al. 2005; Masson et al. 1989) and recently, evidence for C-fiber activation using a 4 Hz
282 sinusoidal (i.e. a full wave-period of 250 ms) current were presented (Jonas et al. 2018). This supports the pulse
283 shape and duration proposed in the present study and further matches early findings on time constant of current
284 increase needed to accommodate sensory fibers (Kugelberg 1944).

285 **Stimulation intensity**

286 The intensity of the exponential pulse is critical for achieving the desired large fiber accommodation and
287 concurrent small fiber activation. Accommodation is different between fiber types and depends on the fiber
288 diameter (Bretag and Stämpfli 1975; Hennings et al. 2005a; Kugelberg 1944) and whether a slowly rising
289 current activates or accommodates a nerve fiber depends on the rate of current increase (Hill 1936). Pain
290 responses to different stimulus intensities were investigated in the current study and identical stimulus-response
291 curves were observed for long exponential and short rectangular single pulse application. Stimulus-response
292 curves with similar pain responses were found for intra epidermal stimulation in a previous study, but the pain
293 ratings did not reach a plateau level as in present study (Lim et al. 2016). The shift in stimulus-response curve
294 towards higher pain ratings for repeated pulses indicated that temporal summation, which most likely reflects

295 gradual depolarization of neurons in the dorsal horn (Sivilotti et al. 1993), played a role in producing maximum
296 pain ratings. This is in accordance with previous studies using repeated electrical stimulation (Arendt-Nielsen et
297 al. 2000). However, it seemed that relatively lower intensity was needed to cause maximum pain using the
298 rectangular pulse compared to the exponential pulse as the curves raised with different rates, but towards
299 identical maximum pain ratings (see Fig. 6). Potential explanations for this difference could be that repeated
300 stimulation of slowly conducting small nociceptive fibers could have led to action potential broadening (Liu et
301 al. 2017) and/or latency jitter at the dorsal horn causing less temporal summation. The absolute current was
302 moreover lower for the exponential pulse compared to rectangular pulse, which may have caused more
303 pronounced habituation (Arendt-Nielsen et al. 2000; Dimitrijević et al. 1972) and less pain facilitation for the
304 lower intensities.

305 **Electrodes and habituation**

306 The different strength-duration curves observed with the pin- and the patch electrodes support the view that the
307 pin electrode mainly activates small fibers and patch electrodes mainly activate large fibers. The results revealed
308 a 2.5-fold larger variance for the pin electrode than the patch electrode. The difference may be explained with
309 different electrode properties. Both electrode-skin contact and size of stimulation area differed between the
310 electrodes. The patch electrode has one relatively large stimulation area whereas the pin electrode is composed
311 of 15 small contact areas. The two electrodes moreover elicit different sensation (Hugosdottir et al. 2017), and it
312 may be speculated whether it is more difficult for the participants to sense the pricking sensation from the pin
313 electrode than the artificial, blunt “shock” like sensation with the patch electrode when low intensities are
314 applied. This factor might explain the different variances, but should however affect the different durations to a
315 similar degree and therefore not affect the curve shape, which is the main outcome of the study. Recently,
316 similar variance variation was observed for perception threshold found with identical electrode types (Hennings
317 et al. 2017). Habituation could also have influenced the variance. The LMM used to analyze the perception
318 threshold showed a linear increase in perception threshold with respect to in which order the pulses were

319 delivered, indicating habituation. Moreover, it was shown that the effect of stimulation order was more
320 pronounced with the pin electrode than with the patch electrode, indicating that small fibers habituated to a
321 larger degree than large fibers. Similar degree of habituation was shown in a study investigating nociceptive
322 detection thresholds to intra-epidermal electro-cutaneous stimulation (van den Berg and Buitenweg 2018). The
323 order of pulse duration and pulse shape was randomized to overcome this limitation.

324 **Limitations**

325 This study was based on subjective perception thresholds with different electrodes in experiment A and
326 subjective pain ratings to different stimulation paradigms in experiment B. The subjective nature of the study is a
327 limitation, but pain is a subjective experience and the method is well acknowledged to investigate pain-related
328 mechanisms in humans (Hennings et al. 2017; Klein et al. 2004). Perception thresholds were used to measure the
329 excitability of small and large fibers with pin- and patch electrodes, respectively. Using such an indirect measure
330 is a limitation of the study, but the perception threshold gives good indication for fiber activation including
331 unknown factors, which most likely are identical between stimulation paradigms. The perception threshold has
332 been used in previous studies to assess membrane properties of nerve fibers (Hennings et al. 2017; Hoberg et al.
333 2019).

334 **Conclusion**

335 This study showed increased perception threshold (accommodation) when slowly rising exponential pulses were
336 delivered with standard patch electrodes, mainly activating large fibers. No threshold increase was observed
337 when identical stimulation pulses were delivered with a pin electrode, mainly activating small fibers. This
338 implies that slowly rising currents can be used to activate small fibers more selectively than standard short
339 pulses. A minimum duration of 20 ms was needed to elevate patch electrode perception thresholds, but longer
340 durations are recommended as the effect increased with increased pulse duration and was most pronounced for
341 100 ms pulse. During repetitive stimulation, co-existing mechanisms might interfere with the small fiber

342 activation during slowly rising pulses and the present study can therefore only support and propose single pulses
343 of slowly increasing exponential pulses for preferential small fiber activation.

344 **Acknowledgements**

345 Center for Neuroplasticity and Pain (CNAP) is supported by the Danish National Research Foundation
346 (DNRF121)

347

348 **5. References**

349

350 **Amaya F, Decosterd I, Samad TA, Plumpton C, Tate S, Mannion RJ, Costigan M, Woolf CJ.** Diversity of
351 expression of the sensory neuron-specific TTX-resistant voltage-gated sodium ion channels SNS and SNS2. *Mol*
352 *Cell Neurosci* 342: 331–342, 2000.

353 **Arendt-Nielsen L, Sonnenborg FA, Andersen OK.** Facilitation of the withdrawal reflex by repeated
354 transcutaneous electrical stimulation: an experimental study on central integration in humans. *Eur J Appl Physiol*
355 81: 165–173, 2000.

356 **Baker M, Bostock H.** Depolarization changes the mechanism of accommodation in rat and human motor
357 neurons. *J Physiol* 411: 545–561, 1989.

358 **van den Berg B, Buitenweg JR.** Analysis of Nociceptive Evoked Potentials during Multi-Stimulus Experiments
359 using Linear Mixed Models. In: *40th Annual International Conference of the IEEE Engineering in Medicine and*
360 *Biology Society (EMBC)*. IEEE, 2018, p. 3048–3051.

361 **Blair NT, Bean BP.** Roles of tetrodotoxin (TTX)-sensitive Na⁺ current, TTX-resistant Na⁺ current, and Ca²⁺
362 current in the action potentials of nociceptive sensory neurons. *J Neurosci* 22: 10277–10290, 2002.

363 **Bostock H, Cikurel K, Burke D, Burke D.** Threshold tracking techniques in the study of human peripheral

364 nerve. [Online]. *Muscle Nerve* 21: 137–58, 1998<http://www.ncbi.nlm.nih.gov/pubmed/9466589> [19 Sep. 2016].

365 **Bretag AH, Stämpfli R.** Differences in action potentials and accommodation of sensory and motor myelinated
366 nerve fibres as computed on the basis of voltage clamp data. *Pflügers Arch Eur J Physiol* 354: 257–271, 1975.

367 **Brindley G, Craggs M.** A technique for anodally blocking large nerve fibres through chronically implanted
368 electrodes. *J Neurol Neurosurg Psychiatry* 43: 1083–1090, 1980.

369 **Burke BYW, Ginsborg BL.** The Electrical Properties of the Slow Muscle Fibre Membrane. *J Physiol* 132: 586–
370 598, 1956.

371 **Dimitrijević MR, Faganel J, Gregorić M, Nathan PW, Trontelj JK.** Habituation: effects of regular and
372 stochastic stimulation. *J Neurol Neurosurg Psychiatry* 35: 234–242, 1972.

373 **Djoughri L, Fang X, Okuse K, Wood JN, Berry CM, Lawson SN.** The TTX-resistant sodium channel Nav1. 8
374 (SNS/PN3): expression and correlation with membrane properties in rat nociceptive primary afferent neurons. *J*
375 *Physiol* 550: 739–752, 2003.

376 **Ebenezer GJ, McArthur JC, Thomas D, Murinson B, Hauer P, Polydefkis M, Griffin JW.** Denervation of
377 skin in neuropathies : the sequence of axonal and Schwann cell changes in skin biopsies. *Brain* 130: 2703–2714,
378 2007.

379 **Fang X, Djoughri L, Black JA, Dib-hajj SD, Waxman SG, Lawson SN.** The Presence and Role of the
380 Tetrodotoxin-Resistant Sodium Channel Na v 1 . 9 (NaN) in Nociceptive Primary Afferent Neurons. 22: 7425–
381 7433, 2002.

382 **Grill WM, Mortimer JT.** Stimulus Waveforms for Selective Neural Stimulation. *IEEE Eng Med Biol Mag* 14:
383 375–385, 1995.

384 **Hennings K, Arendt-Nielsen L, Andersen OK.** Orderly activation of human motor neurons using electrical

385 ramp prepulses. *Clin Neurophysiol* 116: 597–604, 2005a.

386 **Hennings K, Arendt-Nielsen L, Andersen OK.** Breakdown of accommodation in nerve: a possible role for
387 persistent sodium current. *Theor Biol Med Model* 2: 16, 2005b.

388 **Hennings K, Arendt-Nielsen L, Christensen SS, Andersen OK.** Selective activation of small-diameter motor
389 fibres using exponentially rising waveforms: a theoretical study. *Med Biol Eng* 43: 493–500, 2005c.

390 **Hennings K, Frahm KS, Petrini L, Andersen OK, Arendt-Nielsen L, Mørch CD.** Membrane properties in
391 small cutaneous nerve fibers. *Muscle Nerve* 55: 195–201, 2017.

392 **Hill AV.** Excitation and accommodation in nerve. *Proc R Soc Lond B* 119: 305–355, 1936.

393 **Hilliges M, Wang L, Johansson O.** Ultrastructural Evidence for Nerve Fibers Within All Vital Layers of the
394 Human Epidermis. *J Invest Dermatol* 104: 134–137, 1995.

395 **Hoberg TN, Frahm S, Hennings K, Arendt-nielsen L, Mørch CD.** Assessing the modulation of cutaneous
396 sensory fiber excitability using a fast perception threshold technique. *Muscle Nerve* 1–8, 2019.

397 **Hugosdottir R, Mørch CD, Andersen OK, Helgason T, Arendt-Nielsen L.** Evaluating the ability of non-
398 rectangular electrical pulse forms to preferentially activate nociceptive fibers by comparing perception
399 thresholds. *Scand J Pain* 16: 175, 2017.

400 **Inui K, Kakigi R.** Pain perception in humans: use of intraepidermal electrical stimulation. *J Neurol Neurosurg*
401 *Psychiatry* 83: 551–556, 2012.

402 **Inui K, Tran TD, Hoshiyama M, Kakigi R.** Preferential stimulation of A delta fibers by intra-epidermal needle
403 electrode in humans. *Pain* 96: 247–252, 2002.

404 **Jonas R, Namer B, Stockinger L, Chisholm K, Schnakenberg M, Landmann G, Kucharczyk M, Konrad**
405 **C, Schmidt R, Carr R, McMahon S, Schmelz M, Rukwied R.** Tuning in C-nociceptors to reveal mechanisms

406 in chronic neuropathic pain. *Ann Neurol* 1–13, 2018.

407 **Klein T, Magerl W, Hopf HC, Sandkuhler J, Treede RD.** Perceptual correlates of nociceptive long-term
408 potentiation and long-term depression in humans. *J Neurosci* 24: 964–971, 2004.

409 **Koga K, Furue H, Rashid H, Takaki A, Katafuchi T, Yoshimura M.** Selective activation of primary afferent
410 fibers evaluated by sine-wave electrical stimulation. *Mol Pain* 11: 1–11, 2005.

411 **Kugelberg E.** Accommodation in human nerves and its significance for the symptoms in circulatory
412 disturbances and tetany. *Acta Physiol Scand* 8, 1944.

413 **Lelic D, Mørch CD, Hennings K, Andersen OK, Drewes AM, Drewes AM.** Differences in perception and
414 brain activation following stimulation by large versus small area cutaneous surface electrodes. *Eur J Pain* 16:
415 827–37, 2012.

416 **Li C, Bak A.** Excitability Characteristics in a Peripheral of the A- and Nerve. *Exp Neur* 79: 67–79, 1976.

417 **Lim M, Roosink M, Kim JS, Kim HW, Lee EB, Son KM, Kim HA, Chung CK.** Augmented Pain Processing
418 in Primary and Secondary Somatosensory Cortex in Fibromyalgia: A Magnetoencephalography Study Using
419 Intra-Epidermal Electrical Stimulation. *PLoS One* 11, 2016.

420 **Liu PW, Blair NT, Bean BP.** Action Potential Broadening in Capsaicin-Sensitive DRG Neurons from
421 Frequency-Dependent Reduction of Kv3 Current. 37: 9705–9714, 2017.

422 **Lucas K.** On the rate of variation of the exciting current as a factor in electric excitation. *J Physiol* 36: 253–274,
423 1907.

424 **Masson EA, Veves A, Fernando D, Boulton AJM.** Current perception thresholds: a new, quick, and
425 reproducible method for the assessment of peripheral neuropathy in diabetes mellitus. *Diabetologia* 32: 724–
426 728, 1989.

427 **Merrill DR, Bikson M, Jefferys JGR.** Electrical stimulation of excitable tissue: Design of efficacious and safe
428 protocols. *J Neurosci Methods* 141: 171–198, 2005.

429 **Mørch CD, Hennings K, Andersen OK.** Estimating nerve excitation thresholds to cutaneous electrical
430 stimulation by finite element modeling combined with a stochastic branching nerve fiber model. *Med Biol Eng*
431 *Comput* 49: 385–395, 2011.

432 **Mouraux A, Iannetti GD, Plaghki L.** Low intensity intra-epidermal electrical stimulation can activate A δ -
433 nociceptors selectively. *Pain* 150: 199–207, 2010.

434 **Provitara V, Nolano M, Pagano A, Caporaso G, Stancanelli A, Santoro L.** Myelinated nerve endings in
435 human skin. *Muscle Nerve* 35: 767–775, 2007.

436 **Sassen M, Zimmermann M.** Differential Blocking of Myelinated Nerve Fibres by Transient Depolarization.
437 *Pflügers Arch* 341: 179–195, 1973.

438 **Sivilotti LG, Thompson SWN, Woolf CJ, Kingdom U.** Potential Windup in Rat Spinal Neurons In Vitro. *J*
439 *Neurophysiol* 69: 1621–1631, 1993.

440 **Weiss G.** Sur la possibilite de rendre comparables entre eux les appareils servant a l'excitation électrique. *Arch*
441 *Ital Biol* 35: 413–445, 1901.

442 **Xia W, Mørch CD, Andersen OK.** Exploration of the conditioning electrical stimulation frequencies for
443 induction of long-term potentiation-like pain amplification in humans. *Exp Brain Res* 234: 1–11, 2016a.

444 **Xia W, Mørch CD, Andersen OK.** Test-Retest Reliability of 10 Hz Conditioning Electrical Stimulation
445 Inducing Long-Term Potentiation (LTP) -Like Pain Amplification in Humans. *PLoS One* 11: e0161117, 2016b.

446

447

448

449 *Figure 1. The electrodes used in the experiment. Left) Pin electrode is composed of 15 small cathodal pins and a*
450 *concentric anode. Right) The patch electrode cathode*

451 *Figure 2. Examples of the shape of the exponential pulse are shown for durations of 1, 5, 50, and 100 ms. The*
452 *illustrations show the proportion of the maximal stimulation current intensity.*

453 *Figure 3. Re-transformed perception threshold normalized to rheobase (mean \pm standard error) vs. pulse*
454 *duration is shown for a) the patch electrode and b) the pin electrode. Asterisk indicate interactions between*
455 *pulse shape and electrode for the specific durations, * $p < 0.05$, ** $p < 0.01$. Exp = Exponential, Rec =*
456 *rectangular.*

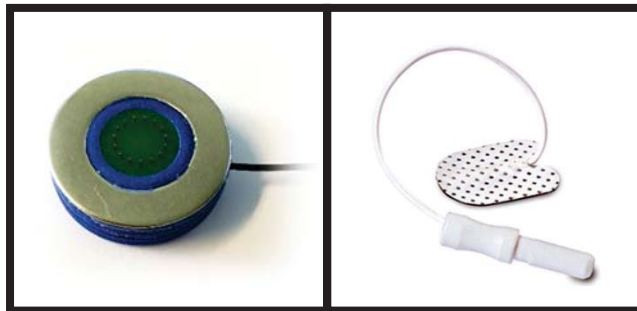
457 *Figure 4. Strength-duration curves (on the left) for the rectangular pulse were used to estimate the rheobase and*
458 *chronaxie, which are presented as median and interquartile range in the table on the right. The perception*
459 *threshold in mA on the y-axis of the strength-duration curve was used to represent the current strength needed*
460 *for activation at different durations with the pin- and the patch electrodes.*

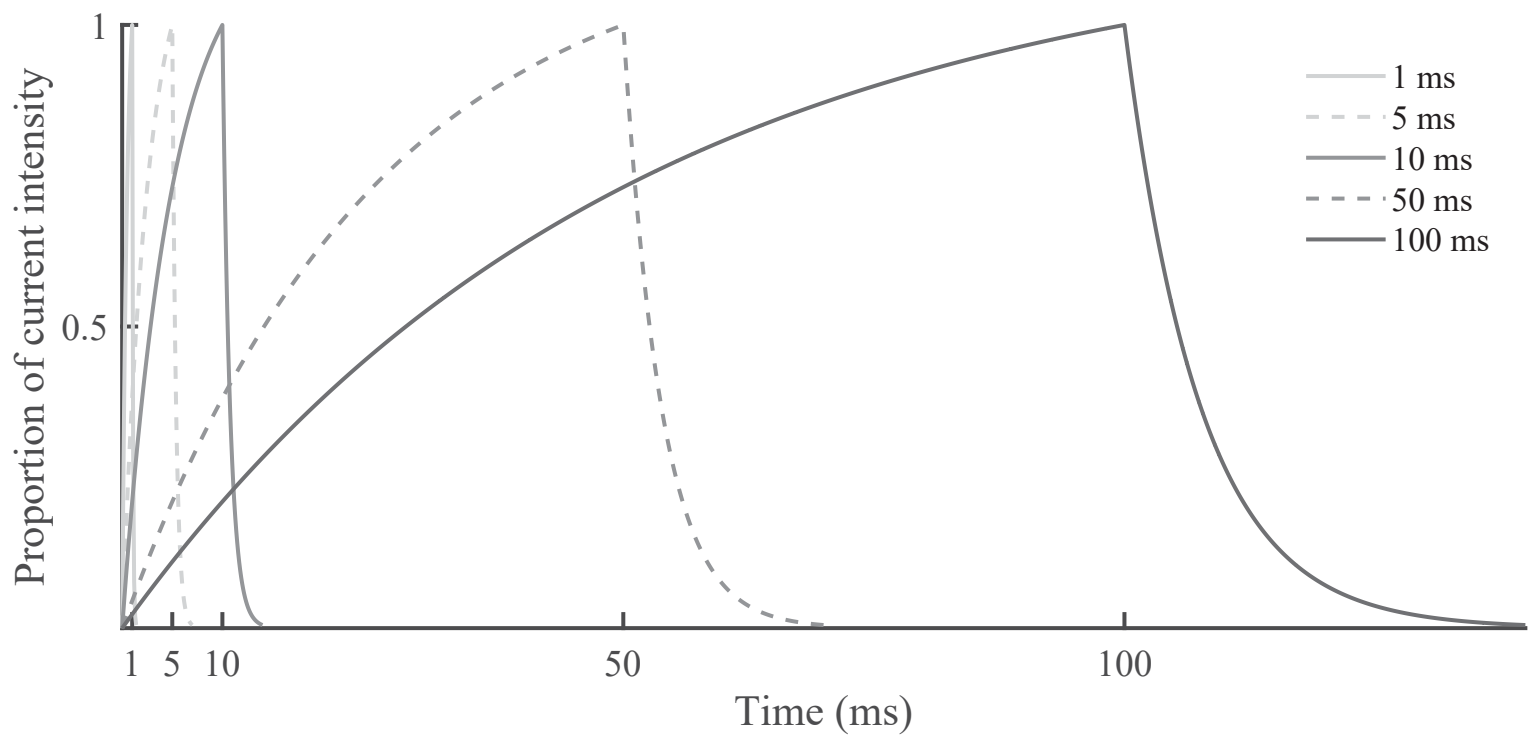
461 *Figure 5: Re-transformed perception thresholds normalized to rheobase (mean \pm standard error) are shown for*
462 *all durations of the exponential pulse for the patch electrode on the left and the pin electrode on the right.*
463 *Asterisk indicate statistically significant interaction between electrode and duration for the pin electrode and $t =$*
464 *1 ms as reference. ** $p < 0.01$, *** $p < 0.001$.*

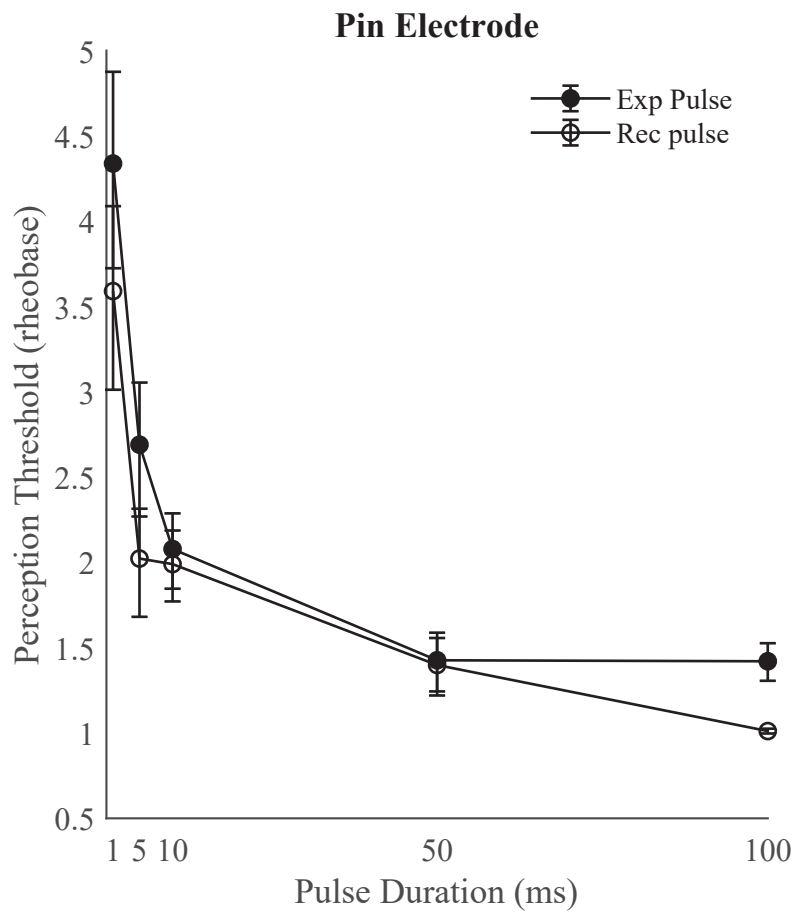
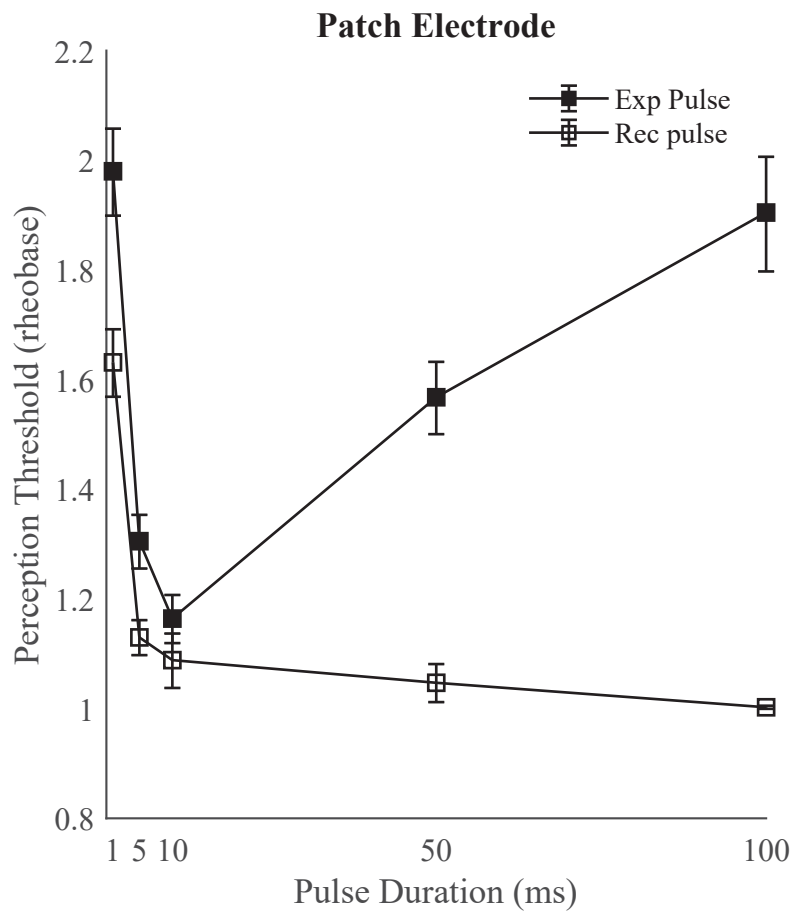
465 *Figure 6. Stimulus-response curves are shown for all paradigms. Pain ratings are shown as mean \pm standard*
466 *error. The fit for sigmoidal curve with 95% confidence interval is added to the plots.*

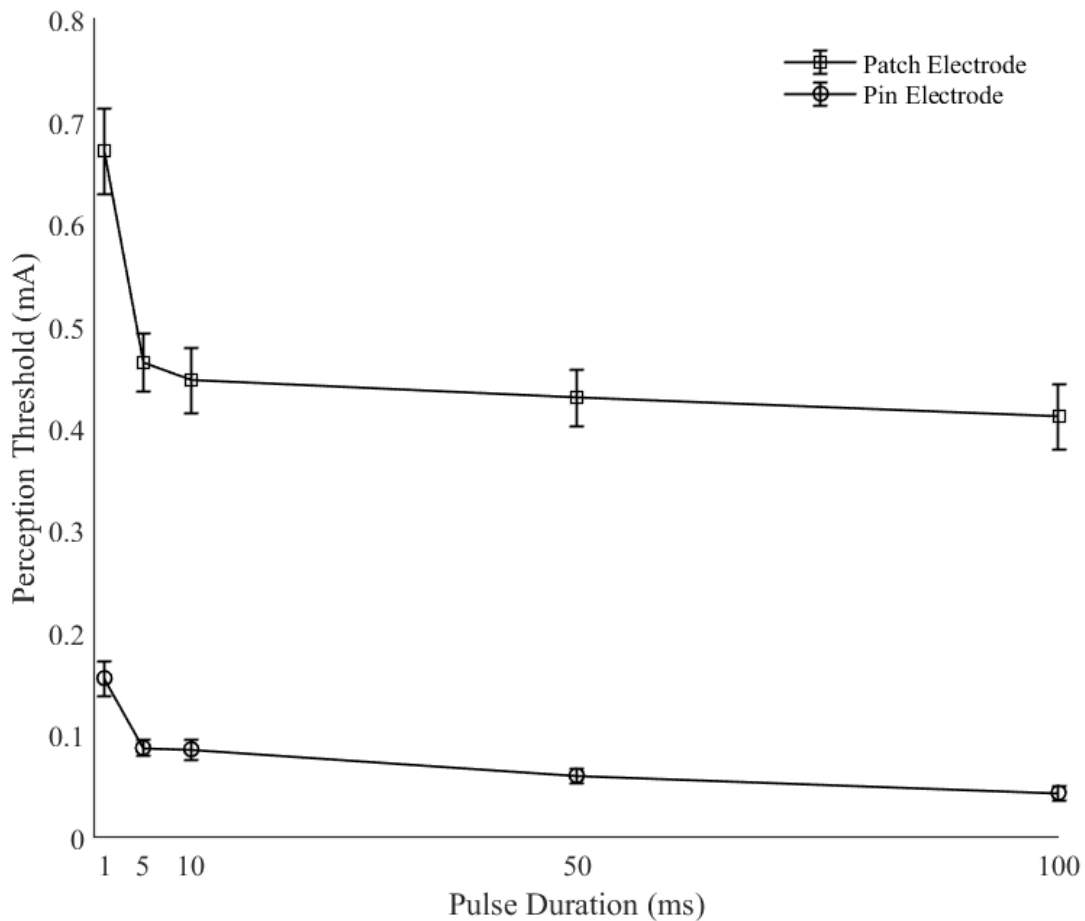
467

468

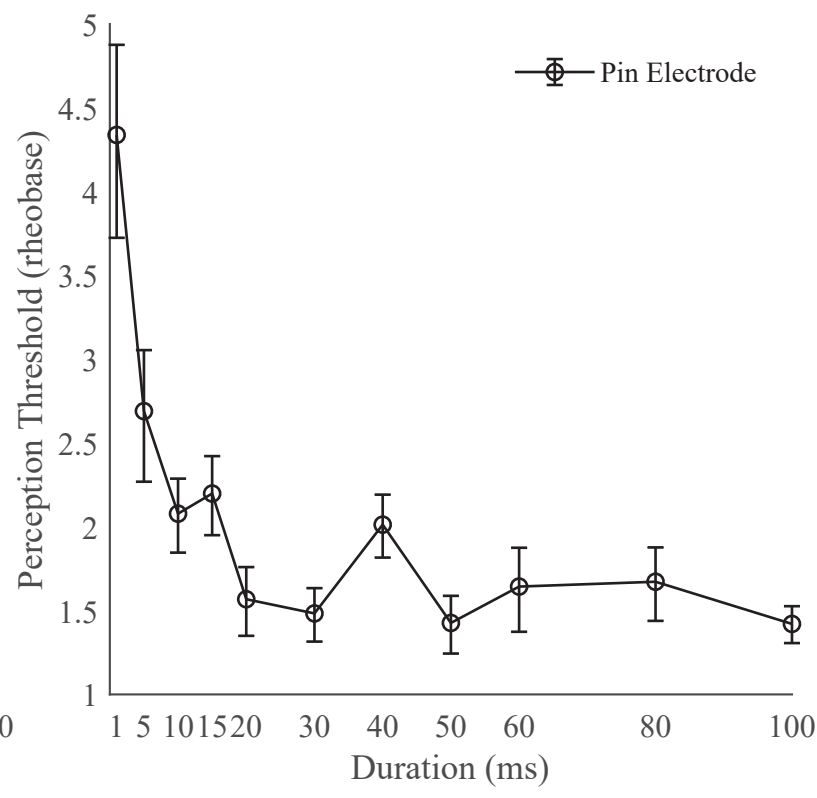
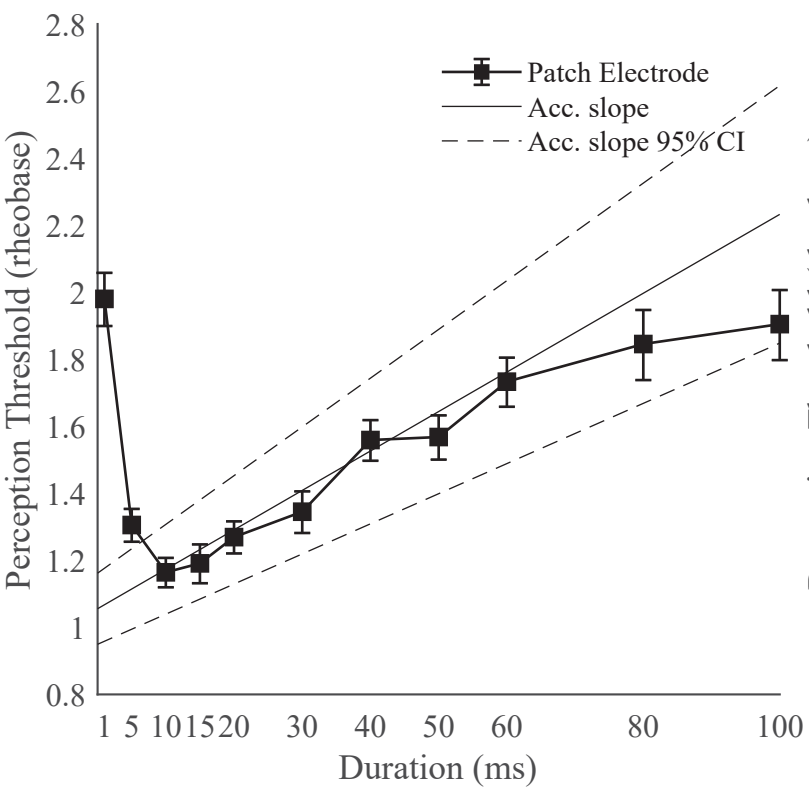








| | Rheobase | |
|------------------------|--------------------|-----------------|
| | Median (mA) | IQR (mA) |
| Pin Electrode | 0.06 | 0.05 |
| Patch Electrode | 0.43 | 0.17 |
| | Chronaxie | |
| | Median (ms) | IQR (ms) |
| Pin Electrode | 1.33 | 2.04 |
| Patch Electrode | 0.594 | 0.19 |



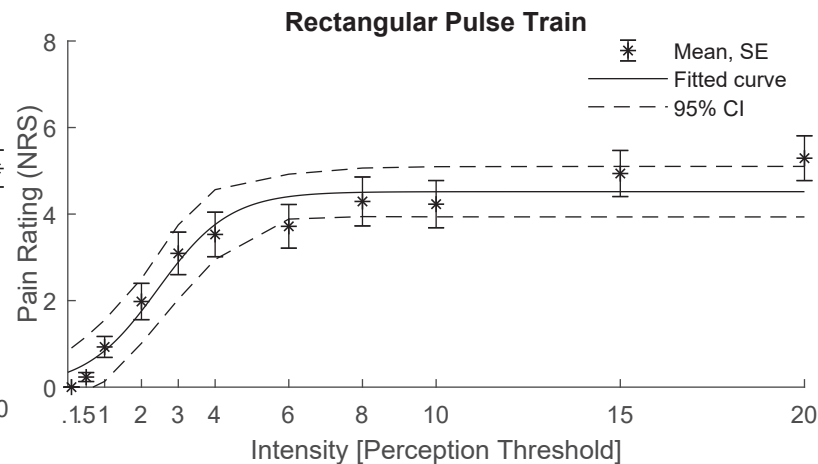
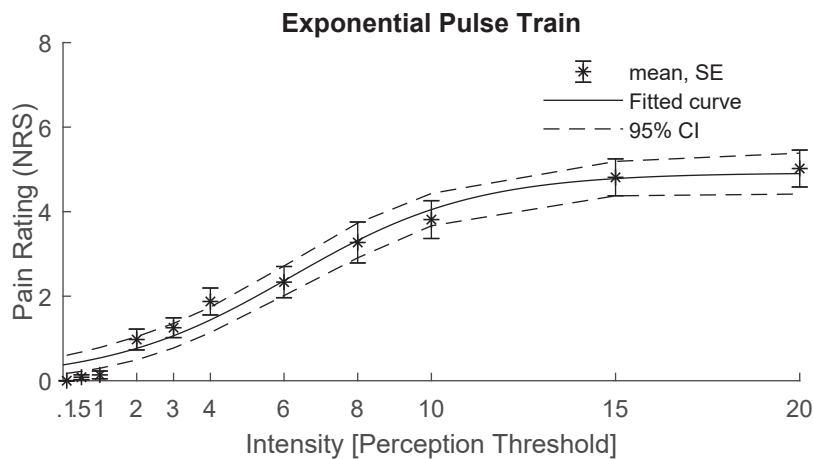
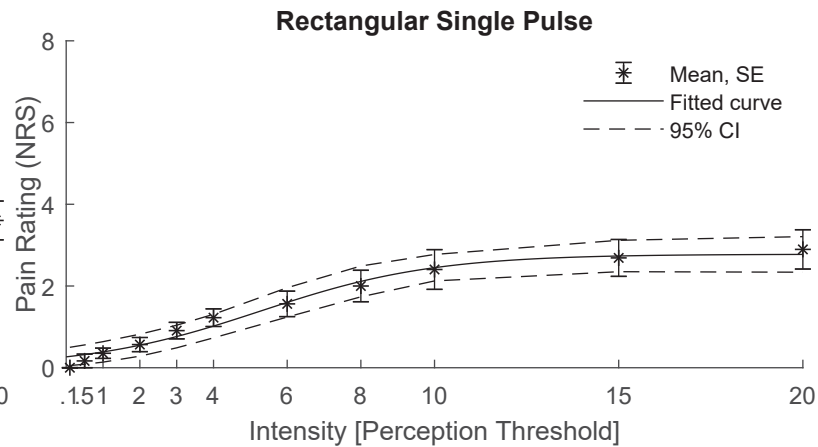
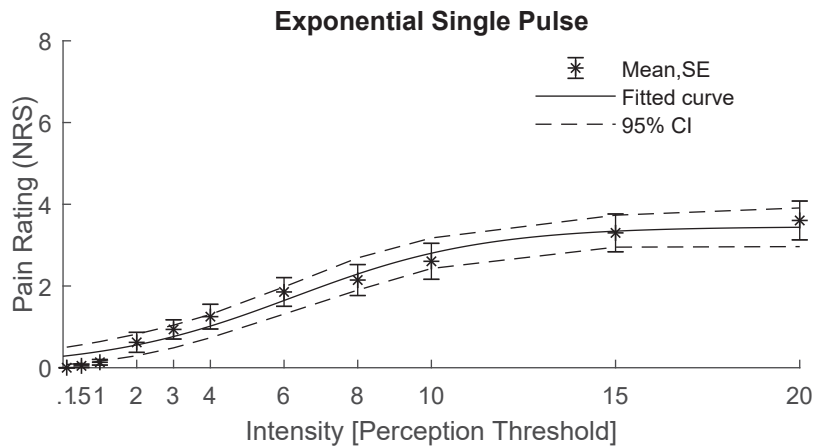


Table 1. Sigmoidal model fit for the pain ratings (NRS). Model coefficients are shown (with 95% confidence interval)

| <i>Paradigm</i> | <i>Adj. R²</i> | <i>A - slope</i> | <i>B – NRS max/2</i> | <i>C – NRS max</i> |
|---------------------------------|---------------------------|-------------------|----------------------|--------------------|
| <i>Exponential single pulse</i> | 0.38 | 0.39 (0.24, 0.54) | 6.24 (4.82, 7.67) | 3.45 (2.96, 3.95) |
| <i>Rectangular single pulse</i> | 0.29 | 0.42 (0.23, 0.62) | 5.29 (3.76, 6.81) | 2.78 (2.33, 3.23) |
| <i>Exponential pulse train</i> | 0.54 | 0.40 (0.29, 0.52) | 6.19 (5.20, 7.19) | 4.92 (4.41, 5.42) |
| <i>Rectangular pulse train</i> | 0.39 | 1.02 (0.56, 1.48) | 2.44 (1.91, 2.97) | 4.52 (4.11, 4.93) |